Hindawi
Journal of Nanomaterials
Volume 2017, Article ID 2849801, 10 pages
https://doi.org/10.1155/2017/2849801

Research Article

Preparation and Characterization of Folate-Targeted Fe_3O_4 Nanoparticle Codelivering Cisplatin and TFPI-2 Plasmid DNA for Nasopharyngeal Carcinoma Therapy

Juan Zhang, Huanhuan Weng, Xiangwan Miao, Quanming Li, Siqi Wang, Huifen Xie, Tao Liu, and Minqiang Xie

Department of Otorhinolaryngology-Head and Neck Surgery, Zhujiang Hospital, Southern Medical University, Guangzhou, China

Correspondence should be addressed to Minqiang Xie; min_qiang_x@hotmail.com

Received 14 July 2017; Accepted 13 November 2017; Published 12 December 2017

Academic Editor: Paulo Cesar Morais

A novel folate (FA) receptor-targeted superparamagnetic Fe_3O_4 nanoparticles (SPIONs) codelivering cisplatin (CDDP) and tissue factor pathway inhibitor-2 (TFPI-2) plasmid DNA (pDNA) was constructed. The core shell nanocomposites (FA-PEG-PEI@SPION-CDDP-TFPI-2) were composed of superparamagnetic Fe_3O_4 core that binds CDDP and TFPI-2 shell that combines with folate-polyethylene glycol-polyethyleneimine (FA-PEG-PEI) via electrostatic interaction. The shell containing FA-PEG-PEI and TFPI-2 plasmid was synthesized through amidation reaction and electrostatic adsorption and the core containing SPION-CDDP was modified by aldehyde sodium alginate. Proton nuclear magnetic resonance and Fourier transform infrared spectra on FA-PEG-PEI polymers showed characteristic peaks of various metabolites in corresponding frequency. Transmission electron microscopy image of FA-PEG-PEI@SPION-CDDP-TFPI-2 nanoparticles demonstrated a near-monodisperse spherical morphology, while dynamic light scattering studies indicated an intensity-average diameter of 149.5 nm. Zeta potential was 14.89 ± 1.83 mv and the final concentration of loaded CDDP was 100 ug/ml. Gel electrophoresis data showed that the nanocomposite would protect TFPI-2 pDNA from being digested by DNases. Compared with CNE-2 cells, the good targetability and better gene transfection efficiency (57.9%) were detected by Prussian blue iron stain and fluorescence analysis in HNE-1 cells in vitro. The results suggested the potential application of FA-PEG-PEI@SPION-CDDP-TFPI-2 as a multifunctional anticancer nanomedicine on targeting therapy for FR positive NPC.

1. Introduction

Nasopharyngeal carcinoma (NPC) is a fairly common malignant tumor in Southern China [1]. The application of intensity modulated radiation therapy (IMRT) has significantly increased the five-year survival rate of NPC patients [2, 3], but it is still unsatisfactory to control the distant metastasis of advanced NPC and severe side effects of radiotherapy [4]. How to improve the therapeutic effect and safety is an urgent problem to be solved on current clinic situation.

In recent decades, significant progress in the development of nanotechnology opens up new possibilities for the development of nanomedicine carried anticancer drug and gene for oncotherapy [5–8]. Liu et al. have synthesized an amphiphilic copolymer (mPEG-PLGA-b-PLL) coated adriamycin and siRNA, which showed a good therapeutic efficiency in huh-7 hepatic carcinoma in mice [9]. Zhu et al. succeed in preparing biodegradable cationic micelles from PDMAEMA-PCL-PDMAEMA triblock copolymers, which not only improved the siRNA and paclitaxel transfection efficiency, but also enhanced the proliferation inhibition effect of the codelivery system on human prostate carcinoma PC-3 cells and human breast cancer MDA-MB-435-GFP cells in vitro [10]. Costa et al. successfully encapsulated pDNA and doxorubicin (DOX) into biocompatible microgels after crosslinking with ethylene glycol diglycidyl ether (EGDE) using an inverse microemulsion polymerization method. The combinatorial delivery of microgels coated pDNA and DOX showed an efficient promotion of cancer Hela cell apoptosis in vitro [11]. In these polymer-drug/gene codelivery systems,

most of combination nucleic acids with cationic hydrophilic shells exhibited excellent biocompatibility and transfection efficiency. However, it required high charge densities and high molecular weights of cationic polymer to condense nucleic acids, which can lead to problems of acute or long-term cells and tissue toxicity [10]. Besides that, significant attention should be afforded to the problem of drug stability and poor drug targeting efficiency.

According to the previous studies, it was demonstrated that folate receptor (FR) is a preferable tumor marker expressed in many tumors such as breast cancer and lung cancer and only in the HNE-1 and Hep-2 cells lines in head and neck cancers, which contribute to the internalization of FA-conjugated nanopolymers into targeted cells [12, 13]. Concomitant radiochemotherapy has become the standard treatment of local advanced NPC. Compared with 5-fluorouracil, bleomycin, and epirubicin, cisplatin (CDDP) was demonstrated to be a better anticancer drug with high activities and durable responses in NPC therapy in clinical studies [14]. Tissue factor pathway inhibitor-2 (TFPI-2) is a serine protease inhibitor contributing to the inhibition of matrix metalloproteinase and the protection from tumor invasion and tumor apoptosis [15]. Our previous study has revealed that TFPI-2 is expressed at a low level in NPC cells and tissues [16]. As proof of concept we use FA as targeting molecules, which conjugated to amino-terminated polyethylene glycol (NH_2-PEG-COOH) and polyethylenimine (PEI) to perform cationic polymers (FA-PEG-PEI) via amidation. Aldehyde sodium alginate modified Fe_3O_4 magnetic particles coated cisplatin (SPION-CDDP) was constructed with the above cationic polymer to obtain composite carriers (FA-PEG-PEI@SPION-CDDP), which then adsorbed TFPI-2 pDNA via electrostatic interaction to obtain the FA-targeted, CDDP, and TFPI-2-coated nanocomposites (FA-PEG-PEI@SPION-CDDP-TFPI-2). In vitro assays indicated that the novel compounds possessed excellent load-carrying capacity and drug stability and showed negligible cytotoxicity and enhanced targetability to FR positive (FR^+) NPC HNE-1 cells.

2. Materials and Methods

2.1. Materials. Folate (FA), dicyclohexylcarbodiimide (DCC), N-hydroxysuccinimide (NHS), dioxotetrahydrofuran, and 4-dimethylaminopyridine (DMAP) were purchased from Aladdin Industrial Co. Ltd. (Shanghai, China). Cisplatin was purchased from Qilu Pharmaceutical Co. Ltd., Shandong, China and dimethyl sulfoxide from J&K Scientific Co. Ltd., Beijing, China. Polyethyleneimine (PEI, Mn = 25 kDa) was purchased from Sigma-Aldrich Co. Ltd. (St Louis, MO, USA). Amino-terminated and hydroxyl polyethylene glycol (NH_2-PEG-OH, Mn = 2 kDa) was obtained from Beijing Chemgenpharma Co. Ltd. (Beijing, China). SPION-CDDP nanoparticles were prepared as we reported previously [17].

pEGFP-C1 plasmid was used for TFPI-2 expressing pDNA that was constructed by GenePharma Co., Ltd. (Suzhou, China), amplified in *Escherichia coli* (Biovector, Beijing, China), and purified using GoldHi EndoFree Plasmid Maxi Kit (CWBIO, Beijing, China). HNE-1 cells, CNE-2 cells, and normal human nasopharyngeal epithelial cells lines (NP-69 cells) were stored in our laboratory. RPMI-1640 culture medium, fetal bovine serum, trypsin (Gibco Grand Island, NY, USA), and cell culture plates (Corning Inc., New York, NY, USA) were purchased. Prussian blue (neutral red) kit was obtained from Solarbio Co. Ltd. (Beijing, China). Celling counting kit-8 was purchased from Dojindo Laboratories (Kumamoto, Japan).

2.2. Methods

2.2.1. Synthesis of FA-PEG-PEI@SPION-CDDP-TFPI-2 Nanocomposites

(1) Preparation of FA-PEG-PEI Cationic Polymer. (I) Terminal carboxyl of FA was activated as follows: DCC (1 g) and NHS (0.575 g) were added to 0.05 g/ml FA solution (20 ml, solvent: DMSO) with TEA (0.5 ml) as acid binding agent, stirring overnight to perform activated terminal carboxyl of FA.

(II) Add NH_2-PEG-OH (4 g) to the above reaction system. After terminal carboxyl of FA reacting with terminal amino group of PEG for 24 h, the mixture was dialyzed (MW = 1000) in deionized water for 3 d and lyophilized to get FA-PEG-OH.

(III) FA-PEG-COOH was prepared by adding DMAP and dioxotetrahydrofuran catalyst with FA-PEG-OH through carboxylation reaction. After that, PEI (4 g) was added to activated FA-PEG-COOH system for 24 h, dialyzed (MW = 25000) for 3 d, and then lyophilized to get FA-PEG-PEI polymer. All the reaction proceeds at room temperature.

(2) Construction of FA-PEG-PEI@SPION-CDDP Nanoparticles. Aldehyde sodium alginate modified Fe_3O_4 superparamagnetic nanoparticles coordinated cisplatin (SPION-CDDP) was performed in our previous study. FA-PEG-PEI polymers were tied to SPION-CDDP to get FA-PEG-PEI@SPION-CDDP nanoparticles through electrostatic interaction. After diluting the above composition to a proper concentration, phenanthroline colourimetry was utilized to measure the Fe concentration by ultra-micro-spectrophotometer (Thermo Scientific Inc., Waltham, MA, USA) at wavelength of 510 nm. O-Phenylenediamine colourimetry was used for determination of the loaded CDDP concentration at wavelength of 703 nm.

(3) TFPI-2 Plasmid Conjugation to Perform FA-PEG-PEI@SPION-CDDP-TFPI-2. TFPI-2 pDNA was electrostatically bound to FA-PEG-PEI@SPION-CDDP in proper proportion, vortexed gently for 5 min at room temperature, and then let stand for 1 h to obtain FA-PEG-PEI@SPION-CDDP-TFPI-2 complexes.

2.2.2. Characterization of FA-PEG-PEI Polymer and FA-PEG-PEI@SPION-CDDP-TFPI-2 Complex

(1) ^{1}HNMR and FT-IR Spectra of FA-PEG-PEI. 5 mg FA-PEG-PEI was diluted with deuteroxide (D_2O) and then characterized by hydrogen nuclear magnetic resonance (^{1}HNMR) spectrum on a Gemini-200 spectrometer (Varian, CA, USA).

FT-IR spectroscopic analyses were carried out by using a Perkin-Elmer spectrophotometer at spectral range of 4000 to 500 cm^{-1} at room temperature.

(2) Physicochemical Property of FA-PEG-PEI@SPION-CDDP-TFPI-2. The morphological structure and the particle size of FA-PEG-PEI@SPION-CDDP-TFPI-2 complexes were studied by transmission electron microscope (TEM) (JEOL, Tokyo, Japan). TEM samples preparation was as follows: diluted sample drops were added to a carbon support film replica, then negatively stained with phosphotungstic acid, and finally dried to visualization. Zeta potential and hydrodynamic diameter of the complexes were received by Malvern laser particle size analyzer (Malvern Instruments Ltd., Worcestershire, UK). Magnetization was measured by a vibrating sample magnetometer (Lake Shore 7410 VSM, America) at the range of −10 kOe to 10 kOe at 25°C.

(3) Gel Electrophoresis of FA-PEG-PEI@SPION-CDDP-TFPI-2 Complexes. The binding abilities of TFPI-2 to FA-PEG-PEI@SPION-CDDP were analyzed by gel electrophoresis restriction assay. First of all, agarose gel (1.0%, w/v) containing ethidium bromide (0.5 ug/ml, Sigma) was solidified for 20 min, which was then placed in the TAE buffer (2 mmol/L EDTA, 40 mmol/L Trisacetate). Section (I): FA-PEG-PEI@SPION-CDDP/TFPI-2 complexes with different mass ratio (1 : 4, 1 : 2, 1 : 1, 2 : 1, 4 : 1) were incubated for 30 min at room temperature and then electrophoresed at 60 mV for 1 h until the separation was achieved. Section (II): to investigate the DNase degradation effects of the composition, FA-PEG-PEI@SPION-CDDP mixed excessive TFPI-2 was incubated with various content of DNase-I (10, 15, 20, and 25 units) for 30 min (120 rpm/min, 37°C), respectively. Afterwards EDTA (4 ul, 250 mM) and SDS solution (4 ul, 10%) were added separately to incubate for additional one hour, and then ran electrophoresis to explore the integrity of DNA. Visualization and photograph capture were accomplished by UV light box using GelDoc system (Synoptics Ltd., UK).

2.2.3. Cytotoxicity Analyses of FA-PEG-PEI/SPION/FA-PEG-PEI@SPION on NP-69 Cells In Vitro. NP-69 cells were cultured onto 96-well plates (2×10^4 cells/well) in Keratinocyte Serum Free Medium (K-SFM) for 24 h at 37°C in a humidified 5% CO2 atmosphere. Once the cell density reached about 70% of the plates, FA-PEG-PEI (100, 200, 400, 800, and 1600 ug/ml) and FA-PEG-PEI@SPION, SPION with various Fe concentration (25, 50, 100, 200, and 400 ug/ml) were added in the plates to cultivate for another 24 h. After that CCK-8 (10 μl) was added to incubate for about 1 h and measured by microplate reader (BioTek Ltd., Winooski, VT, USA) at 450 nm. The cells cultivated with the same amount of PBS was set as negative control. Five multiple holes were set for each sample. Cells Viability Ratio (%) = [OD (experimental) − OD (blank control)]/[OD (negative control) − OD (blank control)] × 100%.

2.2.4. Targeting Transfection Assay of FA-PEG-PEI@SPION-CDDP-TFPI-2 In Vitro. HNE-1 cells (3×10^4 cells/well) and CNE-2 cells (10^4 cells/well) were cultured onto 6-well plates with 10% FBS for 24 h (37°C, 5% CO_2). After that the medium was replaced by folate free RPMI-1640 medium to incubate for 4 h to exclude the effect of exogenous folate in the medium. Thereafter, FA-PEG-PEI@SPION-CDDP-TFPI-2 dissolved folate free RPMI-1640 medium (2 ml/well, the final Fe concentration was 5 μg/ml) was added. After cell transfection test, Prussian blue iron staining was employed for cell iron assessment and expression of GFP was evaluated in optical microscope. Details are as follows.

Prussian Blue Iron Staining. Treated cells (the final Fe concentration was 5 μg/ml) were incubated for another 4 h and then discarded the supernatant. The cells were washed twice with PBS to remove unbonded complexes, fixed with 4% paraformaldehyde, then stained according to Prussian blue (neutral red) kit protocol, and finally photographed under an inverted microscope (Zeiss Ltd, Axio Vert A1, Oberkochen, Baden-Württemberg, Germany).

Expression of GFP. Treated cells (the final Fe concentration was 5 μg/ml) were incubated for another 48 h and then the supernatant was discarded. The cells were washed twice with PBS and then analyzed for GFP expression with a fluorescence microscope (Zeiss Ltd., Axio Vert A1, Oberkochen, Baden-Württemberg, Germany). To analyze the transfection efficiency of the nanocomposites, we, respectively, calculate the number ratio of the transfected cells to total cells within five randomly selected fields under the microscope and then strike an average.

2.2.5. Statistical Analysis. All data were analyzed by SPSS 20.0 software and shown as mean ± SD. Student's t-test was used to compare the means of two independent samples. Differences were considered to be significant when the P value was less than 0.05 ($P < 0.05$).

3. Results and Discussion

Compared with single chemotherapy or radiotherapy, concurrent radiochemotherapy with or without adjuvant chemotherapy has been proved to better contribute to the treatment of advanced NPC with stages T1-2N2-3 and T3-4N1-3 [18]. However, the nonuniform treatment program and the lack of tissue targeting are problems that need to be addressed. Therefore, gene targeting therapy has come into the spotlight in team researches and clinical trials [19–21]. Our previous studies have, respectively, developed a cyclodextrin-poly derivative [22] and a folate-targeted cationic copolymer [23] to carry docetaxel and MMP siRNA plasmid for better anti-NPC treatment. In vitro assay demonstrated the superiority of the composites in promoting tumor cell apoptosis and inhibiting their invasion ability. In vivo trials indicated that the composites showed negligible cytotoxicity and good blood compatibility. However, the former synthetic polymer was lack of targetability, which easily led to surrounding healthy tissues damage. Additionally, MMP-9 gene silencing suggested poor inhibition in NPC. In our research, SPION served as the core of nanocarrier. As a result, nanodrugs uptake by tumors could be easily detected by MRI

and Prussian blue iron staining. TFPI-2 plasmid encoding GFP was capable of inhibiting a variety of MMPs and thus promoted the anticancer effect. It was also easier to observe the gene transfection efficiency with GFP expression. Cationic polymer PEI was an efficient nonviral gene delivery agent, which could stably adsorb and condense pDNA and then bind to negatively charged targeting cell surfaces. However, the aggregation of excess amino groups provoked cytotoxicity in vivo, which limited its application [24]. To overcome such problems, we considered the cross-coupling reaction between the above cationic carriers and nonionic water-soluble polymers PEG to increase the solubility and decrease aggregation of the composites. Besides that, the combination between CDDP and aldehyde sodium alginate modified SPION is more capable of adsorbing PEG modified PEI via electrostatic interaction due to the improved biocompatibility, water-solubility, and longer circulation time in blood. Meanwhile, the targeting FA-PEG-PEI was prepared by amidation reaction between the carboxyl groups of FA and amino groups of NH_2-PEG-OH. Finally, FA-PEG-PEI@SPION-CDDP-TFPI-2 nanocomplex was performed by linking FA-PEG-PEI with SPION-CDDP and CDDP according to appropriate proportion. In vitro assay demonstrated the superiority of the nanocomplex in specific targetability for FR^+ tumors.

3.1. Characterization of FA-PEG-PEI Polymer and FA-PEG-PEI@SPION-CDDP-TFPI-2 Nanocomplex

3.1.1. ^{1}HNMR and FT-IR Spectra of FA-PEG-PEI Polymer. ^{1}H NMR was determined to confirm the synthesis of FA-PEG-PEI (the spectrum and relevant chemical structural formula were shown in Figure 1). The characteristic peaks from 2.0 to 3.0 ppm (k, j) were attributed to -CH_2CH_2NH- group of PEI, the peaks at 3.66 ppm (h) were referred to -CH_2CH_2O- group of PEG, and the peaks from 6.5 to 9.0 ppm (a, b, c) were related to the H protons of benzene ring in FA [25]. The data suggested a successful combination of FA-PEG-PEI.

The possible functional groups responsible for the synthesis of FA-PEG-PEI were further confirmed by FT-IR spectroscopy. Meanwhile, the FT-IR spectra of FA, NH_2-PEG-OH, and NH_2-PEG-COOH were also examined. The terminal hydroxyl groups of NH_2-PEG-OH were of carboxylation and then combined with the amino groups of PEI via amidation reaction. As shown in Figure 2, the FT-IR spectra of terminal hydroxyl groups of (b) NH_2-PEG-OH showed the presence of stretching vibration peak of -OH at 3440 cm^{-1}, which shifted to a new stretching vibration peak of -C=O at 1629 cm^{-1} in (c) NH_2-PEG-COOH after carboxylation. The FT-IR spectra of (d) FA-PEG-PEI displayed a broad peak at 3350–3250 cm^{-1}, which refers to -NH_2 and -NH- groups of PEI. The peaks at 1606–1460 cm^{-1} correspond to the benzene ring of FA. In addition, the peak at 1110 cm^{-1} is attributed to the symmetrical stretching vibration of -C-O-C- group in PEG, which declares the conjugation of FA-PEG-PEI.

3.1.2. Gel Electrophoresis of FA-PEG-PEI@SPION-CDDP-TFPI-2 Complexes. The FA-PEG-PEI@SPION-CDDP was constructed with SPION-CDDP (core) and FA-PEG-PEI (shell). Numerous detached electropositive amino groups in the shell covered SPION-CDDP nanoparticles were able to electrostatically adsorb electronegative TFPI-2 pDNA. To explore the binding ability of FA-PEG-PEI@SPION-CDDP with TFPI-2 pDNA, gel electrophoresis was observed in Figure 3(a). It was found that with the increasing mass ratio of FA-PEG-PEI@SPION-CDDP/TFPI-2 {Figure 3(a)~B (1 : 4) → C (1 : 2) → D (1 : 1)}, more TFPI-2 was blocked in sample well. When the mass ratio was equal to or more than 2 (Figure 3(a)~E), TFPI-2 pDNA was restricted completely in the well, indicating entirely adsorption and encapsulation by FA-PEG-PEI@SPION-CDDP. As a result, the relative mass ratio was determined as 2 : 1 to synthesize the final complex. To investigate the protection of TFPI-2-loaded complex (FA-PEG-PEI@SPION-CDDP-TFPI-2) against DNase-I degrading, FA-PEG-PEI@SPION-CDDP was mixed with overdose TFPI-2, then various content of DNase-I was added to run electrophoresis. As shown in Figure 3(b), compared with TFPI-2 migration without DNase-I in Figure 3(a)~B, the more DNase-I was added, the more detached TFPI-2 was degraded with more fade band of TFPI-2 migration. When DNase-I was equal to or higher than 15 units, the detached TFPI-2 (Figure 3(b)~J, K) was entirely digested except for the sample well. This evidence shed light on the enzymatic hydrolysis of DNase-I in TFPI-2 pDNA and indicated that FA-PEG-PEI@SPION-CDDP is feasible in adsorbing TFPI-2 and protecting pDNA from degradation. Thus pDNA could avoid digestion by DNase in media or blood before reaching the targeted cells, leading to an efficient transfection in tumors.

3.1.3. Physicochemical Property of FA-PEG-PEI@SPION-CDDP. Proper particle diameter [25, 26] and positive surface charge of nanodrug play an important role in cellular uptake of drug and enhancement target-oriented effects [17]. The particle size of FA-PEG-PEI@SPION-CDDP-TFPI-2 complexes was determined using TEM (Figure 4(a)). TEM micrograph illustrated monodisperse spherical particles with an average diameter of 55.2 ± 8.4 nm, the sizes of which contribute to avoiding phagocytosis by macrophages, renal excretion, and aggregation in the bone marrow. There were several SPION particles at an average diameter of 8 nm arranged as a ring inside the complex. Negligible sedimentation was observed in the complex liquid with one-year observation, which suggested excellent stability of the system. The TEM EDS in Figure 4(b) verified the presence of Pt and Fe elements in FA-PEG-PEI@SPION-CDDP-TFPI-2 complexes, suggesting a potent combination between CDDP and SPION. The Fe content and CDDP loading amount were 5.35 mg/ml and 100 ug/ml, respectively, as counted according to corresponding standard curves by colorimetry.

The average hydrodynamic diameter of FA-PEG-PEI@SPION-CDDP-TFPI-2 complex was 149.5 nm (Figure 5(a)) as determined by DLS, which showed larger diameter than that of TEM. This could be attributed to the swelling and stretching of chemical group on the surface of the final complex in solution. Besides, the Vander Waals force between cationic group and hydrogen-bonds could also effect. As

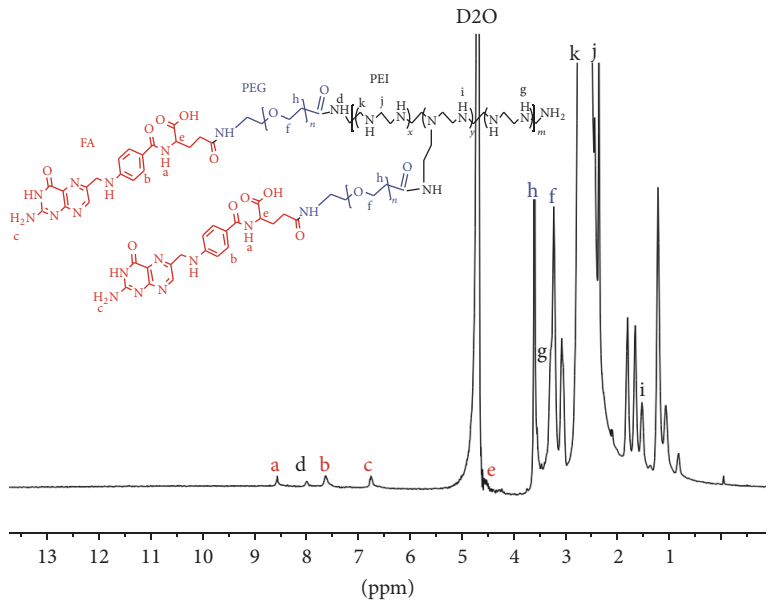

Figure 1: ^{1}H NMR spectrum of FA-PEG-PEI polymer (D_2O).

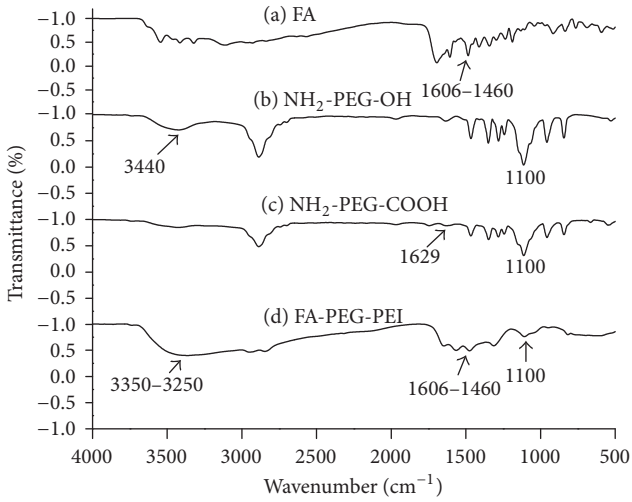

Figure 2: FT-IR spectra of (a) FA, (b) NH_2-PEG-OH, (c) NH_2-PEG-COOH, and (d) FA-PEG-PEI.

shown in Figure 5(b), Zeta potential was 14.89 ± 1.83 mV, which indicated that the compounds were positively charged, which is beneficial to uptake by negatively charged cell surfaces of NPC.

The saturation magnetization (Ms) was determined by vibrating sample magnetometer (VSM) as shown in Figure 6(a). According to the saturation magnetization curves, (I) SPION (30.22 emu/g) owned the optimal Ms, followed by (II) SPION-CDDP (26.76 emu/g) and (III) FA-PEG-PEI@SPION-CDDP-TFPI-2 (22.89 emu/g). Coercivity and remanence were zero, indicating superparamagnetism of the above nanoparticles. In addition, the three kinds of nanoparticles (Figure 6(b)) were monodisperse and stable in water after standing for 1 year. After magnets were attracted with an external magnetic field for 24 h, the nanoparticles were capable of directional magnetic adsorption as shown in Figure 6(c), which declared sufficient magnetization value for biomedical application [27] such as magnetic targeting [28] and magnetic hyperthermia.

3.2. Cytotoxicity Analyses of FA-PEG-PEI/SPION/FA-PEG-PEI@SPION on NP-69 Cells In Vitro. CCK-8 assay was carried out to observe the cytotoxicity of FA-PEG-PEI/SPION/FA-PEG-PEI@SPION in normal human nasopharyngeal epithelial cells (NP-69 cells). Figure 7 showed that the cell viability in FA-PEG-PEI group was reduced following the increasing Fe concentration. The vitality sharply declined to 5% when the Fe concentration was up to 400 ug/ml, which shed light on high toxicity of FA-PEG-PEI group, while free SPION particles exhibited little toxicity. The possible cause of the problem is that the unblocked amino group of PEI~ [29, 30] destroyed NP-69 cell surface and further increased permeability of cell membranes. Compared with FA-PEG-PEI polymer (the Fe concentration was 400 ug/ml), FA-PEG-PEI@SPION nanovector displayed far higher cells viability (82%), indicating lower cytotoxicity. The possible reason would be that the free cationic amino of FA-PEG-PEI may be properly condensed after being capsulated by SPION, preventing it from exposure to the NP-69 cell membrane.

3.3. Targeting Transfection Assay of FA-PEG-PEI@SPION-CDDP-TFPI-2 Nanocomposites In Vitro. Internalization of FA-PEG-PEI@SPION-CDDP-TFPI-2 nanocomposites into targeted cells only occurred in FR^+ cells. The nanocomposites were transfected into FR^+ HNE-1 cells and FR^- CNE-2 cells [12] for 4 h to investigate the FA targetability of folate-conjugated nanoparticles via Prussian blue staining. As shown in Figure 8, HNE-1 cells (Figure 8(b)) contained more blue staining granules inside than CEN-2 cells (Figure 8(a)).

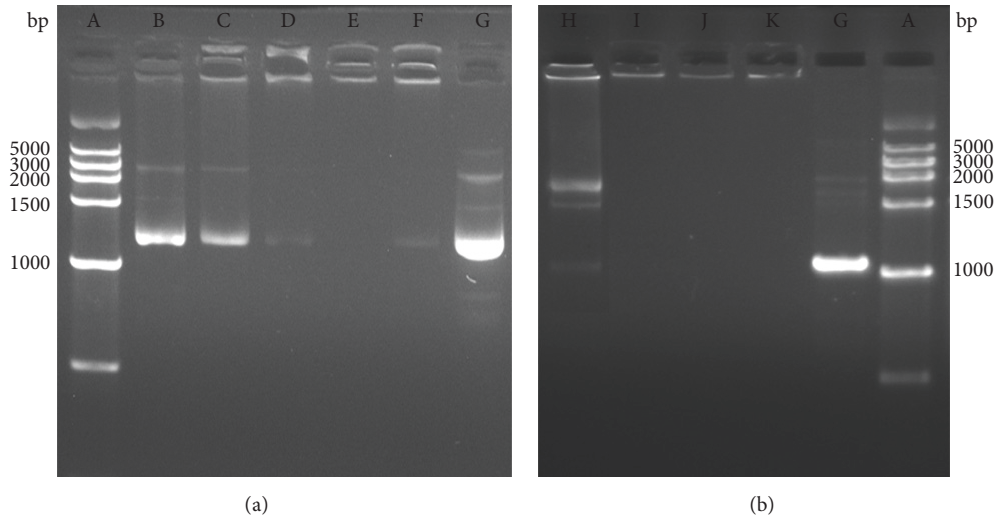

Figure 3: (a) Agarose gel electrophoresis restriction assay of FA-PEG-PEI@SPION-CDDP-TFPI-2 at various mass ratio {B (1 : 4), C (1 : 2), D (1 : 1), E (2 : 1), F (4 : 1)}. (b) Dnase-I degradation assay of FA-PEG-PEI@SPION-CDDP-TFPI-2 (overdose TFPI-2) with DNase-I at various contents (H, I, J, K = 10, 15, 20, 25 units). (A) Marker; (G) naked TFPI-2 pDNA.

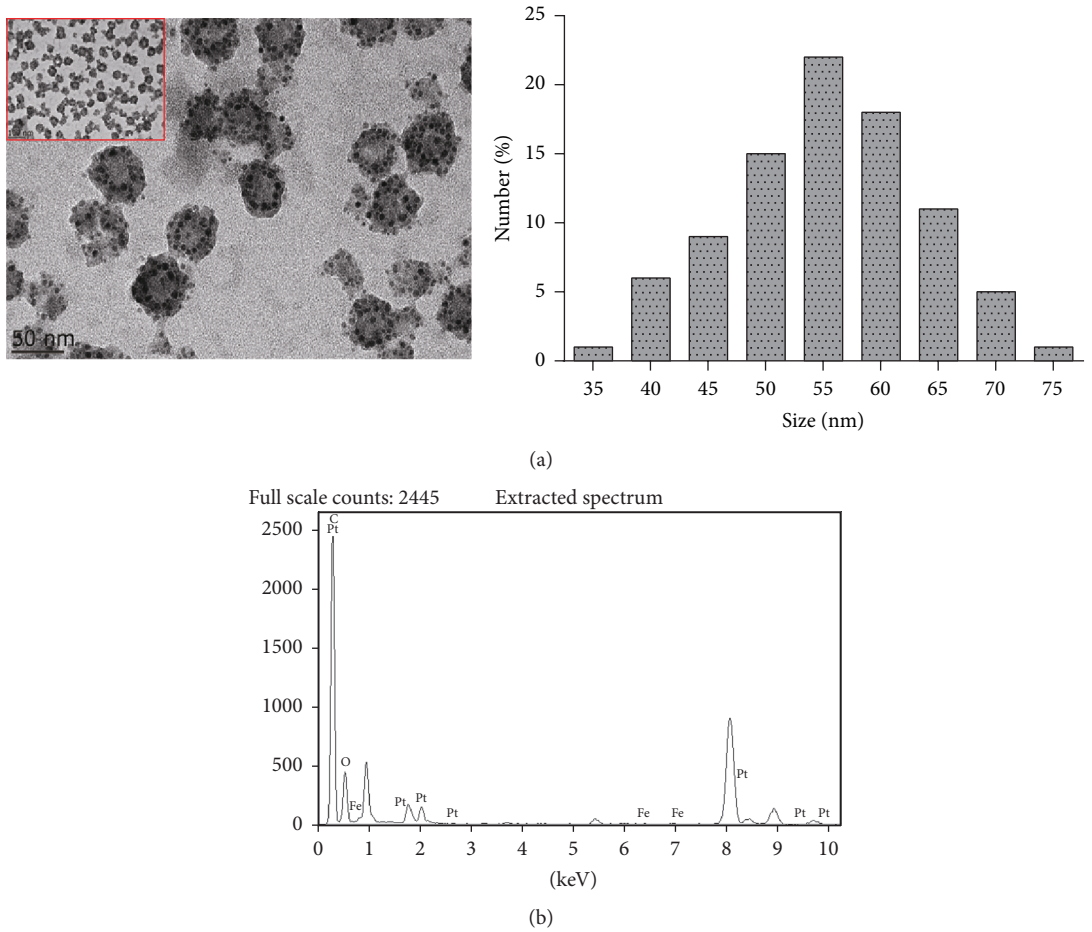

Figure 4: (a) TEM image and particle size distribution of FA-PEG-PEI@SPION-CDDP-TFPI-2 complexes. (b) The TEM EDS of FA-PEG-PEI@SPION-CDDP-TFPI-2 complexes.

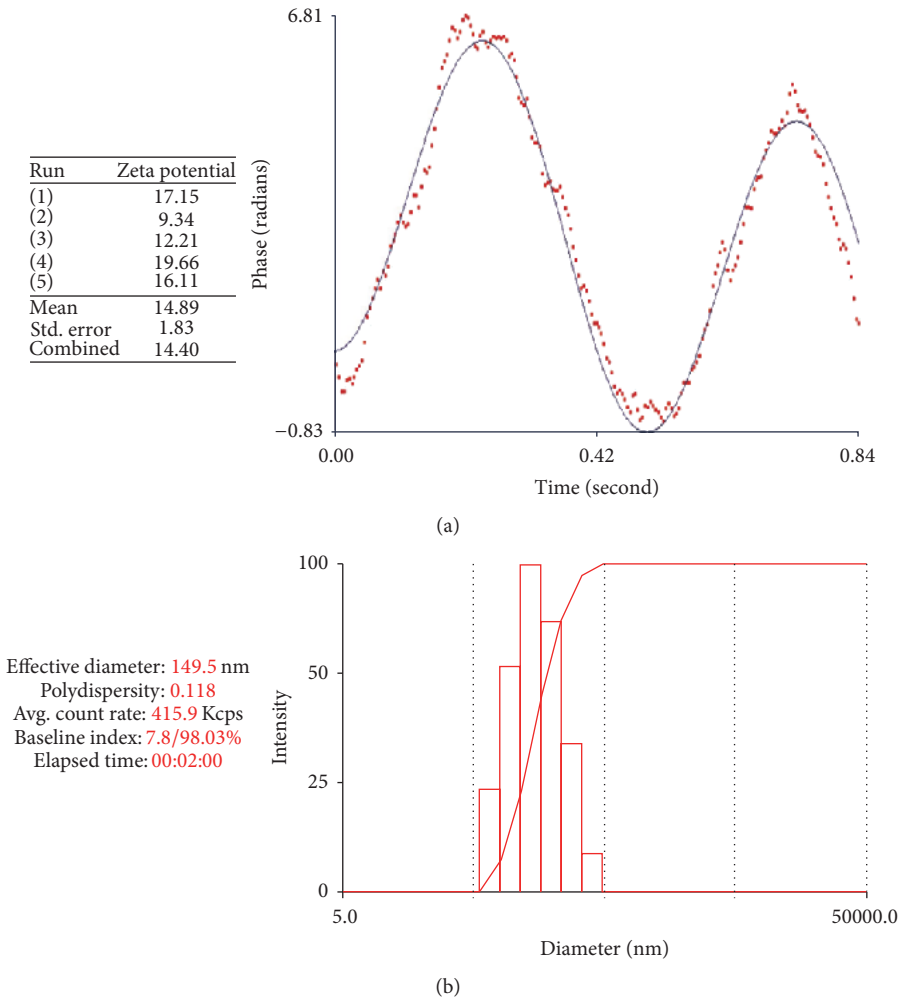

Figure 5: The average hydrodynamic diameter (a) and Zeta potential (b) of FA-PEG-PEI@SPION-CDDP-TFPI-2.

The former held a higher transfected cells efficiency (75.8%) in comparison with the latter (16.5%), which suggested that the FA-PEG-PEI@SPION-CDDP-TFPI-2 possessed a good targetability of HNE-1 cells due to the highly expression of folate receptor on HNE-1 surface. As a result, the FA-conjugated nanoparticles could bind to FR^+ HNE-1 cells specifically rather than FR^- CNE-2 cells as described above.

The GFP expression was observed via fluorescence microscope after the same nanoparticles above had been transfected into cells for 48 h. The amount of GFP expression in HNE-1 cells (Figure 8(f)) is more than that in CNE-2 cells (Figure 8(d)), which meant higher transfection efficiency (57.9%) of the final nanoparticles in HNE-1 cell ($P = 0.0009$, $***$ means significant, and $P < 0.01$) compared with CNE-2 (13.5%) (Figure 8(g)). The outcome consisted of that of Prussian blue staining assay. Interestingly, there was not statistic difference of transfected efficiency between Prussian blue staining assay (75.8%) and GFP expression (57.9%) in the same HNE-1 cell line ($P = 0.0836$, NS means nonsignificant, and $P > 0.05$), which further proved the integrity of our FA-targeted drug/gene loaded nanoparticles.

The experiments had demonstrated that FA-PEG-PEI@SPION-CDDP-TFPI-2 composites held a good targetability and gene transfection efficiency in FR^+ HNE-1 cells. Therefore, the anticancer drugs were more accurately targeting NPC cells with FA-targeted endocytosis and the cellular content of CDDP and TFPI-2 would significantly increase, resulting in a better anticancer effect.

4. Conclusion

In an effort to reduce toxicity, a novel cationic polymer (FA-PEG-PEI) was successfully developed via amidation reaction. Aldehyde sodium alginate modified SPION coated cisplatin (SPION-CDDP) was constructed with the above cationic polymer and TFPI-2 pDNA via electrostatic interaction to obtain FA-PEG-PEI@SPION-CDDP-TFPI-2. In vitro assays demonstrated good stability and water-solubility of the FA-targeted complexes codelivering cisplatin and TFPI-2 pDNA. In addition, it showed an obvious targeting ability and great gene transfection efficiency with FR^+ tumor. Success in the syntheses of the target therapeutic agents opens up new

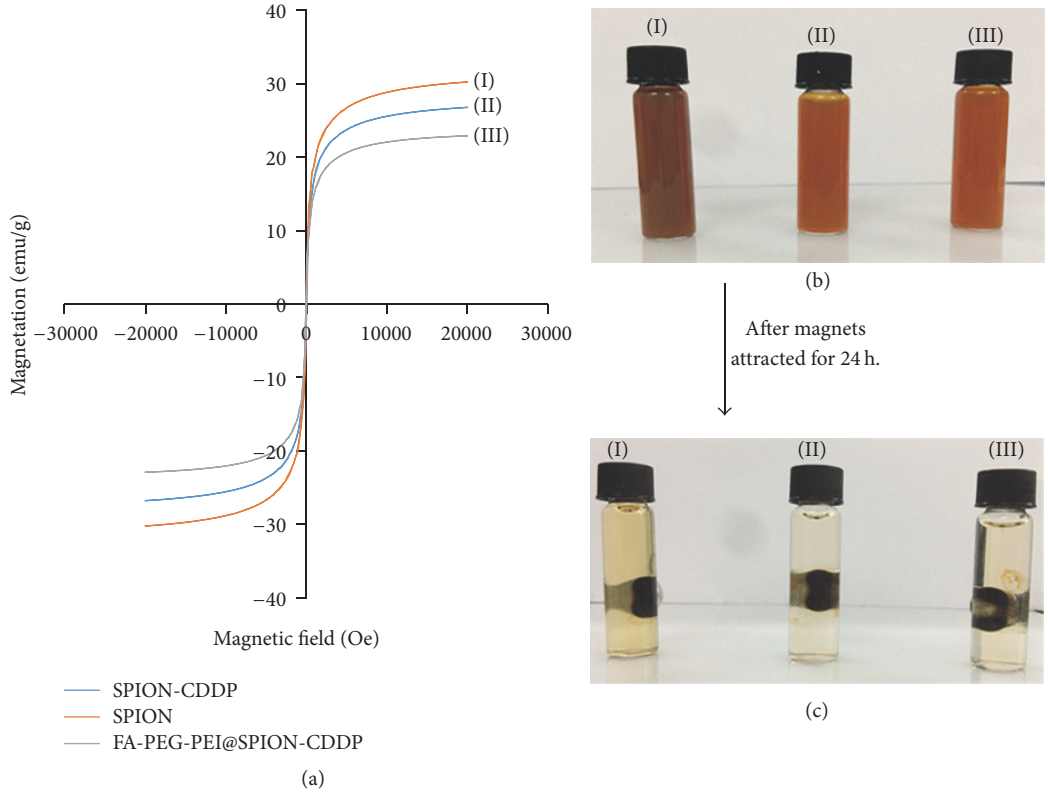

Figure 6: The magnetization analysis of (I) SPION, (II) SPION-CDDP, and (III) FA-PEG-PEI@SPION-CDDP. (a) Saturation magnetization curves of various nanoparticles. (b) Stable and monodisperse status of the above nanoparticles. (c) Nanoparticles were directional attracted with an external magnetic field.

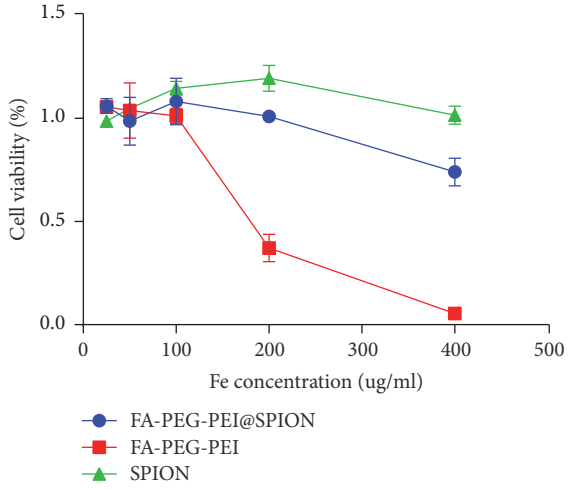

Figure 7: Cytotoxicity analyses on NP-69 cells.

possibilities for clinical tumor treatment and reduction in adverse effects.

Conflicts of Interest

The authors declare that they have no conflicts of interest.

Acknowledgments

This study was financially supported by the National Natural Science Foundation of China (nos. 81372477, 81573000, and 81673013) and the Science and Technology Project of Guangdong Province, China (Grant no. 2017B080701038).

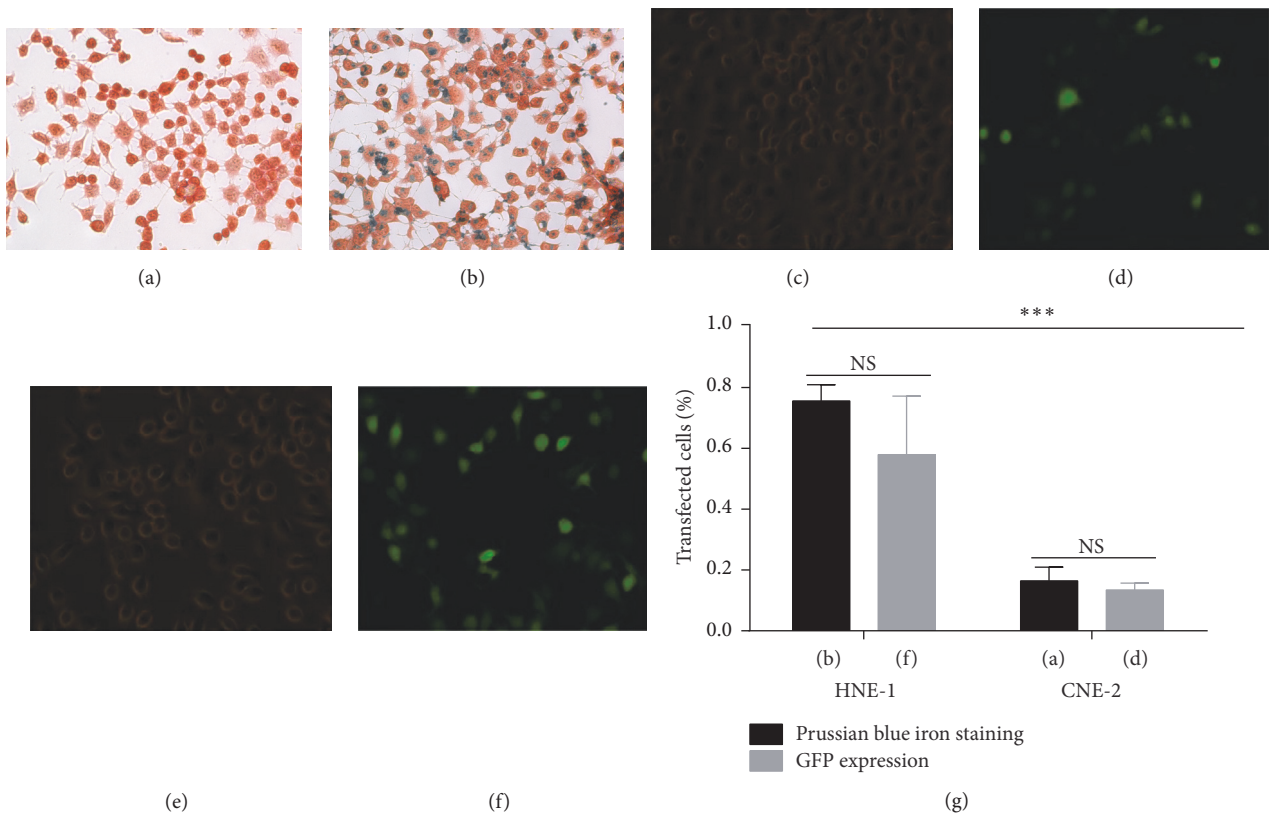

Figure 8: (a-b) Prussian blue staining in FR^- CNE-2 cells (a) and FR^+ HNE-1 cells (b). (c–f) GFP expression in FR^- CNE-2 cells (c, d) and FR^+ HNE-1 cells (e, f); (c/e) were under white light, and (d/f) were under blue excitation light. (g) The account of transfected cells (data was expressed as mean ± SD, $n = 5$, NS means nonsignificant and $P > 0.05$, and $***$ means significant and $P < 0.01$ by t-test). All cells were treated with FA-PEG-PEI@SPION-CDDP-TFPI-2 (Fe concentration = 5 ug/ml; 200x).

The authors also appreciate the technical help of Professor Liming Zhang, Xueqing Xu, and Xiaoyi Fu.

References

[1] M. C. Yu and J. M. Yuan, "Epidemiology of nasopharyngeal carcinoma," *Seminars in Cancer Biology*, vol. 12, no. 6, pp. 421–429, 2002.

[2] M.-X. Zhang, J. Li, G.-P. Shen et al., "Intensity-modulated radiotherapy prolongs the survival of patients with nasopharyngeal carcinoma compared with conventional two-dimensional radiotherapy: A 10-year experience with a large cohort and long follow-up," *European Journal of Cancer*, vol. 51, no. 17, pp. 2587–2595, 2015.

[3] K. R. Wei, R. S. Zheng, S. W. Zhang, Z. H. Liang, Z. X. Ou, and W. Q. Chen, "Nasopharyngeal carcinoma incidence and mortality in China in," *ChinJCancer*, vol. 33, no. 8, pp. 381–387, 2010.

[4] X. Sun, S. Su, C. Chen et al., "Long-term outcomes of intensity-modulated radiotherapy for 868 patients with nasopharyngeal carcinoma: an analysis of survival and treatment toxicities," *Radiotherapy & Oncology*, vol. 110, no. 3, pp. 398–403, 2014.

[5] J. Panyam and V. Labhasetwar, "Biodegradable nanoparticles for drug and gene delivery to cells and tissue," *Advanced Drug Delivery Reviews*, vol. 55, no. 3, pp. 329–347, 2003.

[6] I. I. Slowing, J. L. Vivero-Escoto, C. W. Wu, and V. S. Y. Lin, "Mesoporous silica nanoparticles as controlled release drug delivery and gene transfection carriers," *Advanced Drug Delivery Reviews*, vol. 60, no. 11, pp. 1278–1288, 2008.

[7] Z. Liu and N. Zhang, "PH-sensitive polymeric micelles for programmable drug and gene delivery," *Current Pharmaceutical Design*, vol. 18, no. 23, pp. 3442–3451, 2012.

[8] W. Chen, F. Meng, R. Cheng, C. Deng, J. Feijen, and Z. Zhong, "Advanced drug and gene delivery systems based on functional biodegradable polycarbonates and copolymers," *Journal of Controlled Release*, vol. 190, pp. 398–414, 2014.

[9] P. Liu, H. Yu, Y. Sun, M. Zhu, and Y. Duan, "A mPEG-PLGA-b-PLL copolymer carrier for adriamycin and siRNA delivery," *Biomaterials*, vol. 33, no. 17, pp. 4403–4412, 2012.

[10] C. Zhu, S. Jung, S. Luo et al., "Co-delivery of siRNA and paclitaxel into cancer cells by biodegradable cationic micelles based on PDMAEMA-PCL-PDMAEMA triblock copolymers," *Biomaterials*, vol. 31, no. 8, pp. 2408–2416, 2010.

[11] D. Costa, A. J. M. Valente, M. G. Miguel, and J. Queiroz, "Plasmid DNA microgels for drug/gene co-delivery: a promising approach for cancer therapy," *Colloids and Surfaces A: Physicochemical and Engineering Aspects*, vol. 442, pp. 181–190, 2014.

[12] M. Xie, H. Zhang, Y. Xu et al., "Expression of folate receptors in nasopharyngeal and laryngeal carcinoma and folate receptor-mediated endocytosis by molecular targeted nanomedicine,"

International Journal of Nanomedicine, vol. 8, pp. 2443–2451, 2013.

[13] X. M. Z. Hongzheng, "Expression of folate receptor in the tissues and cells of nasopharyngeal carcinoma," *China Journal of Modern Medicine*, vol. 19, no. 6, p. 8, 2009.

[14] A. Taamma, A. Fandi, N. Azli et al., "Phase II trial of chemotherapy with 5-fluorouracil, bleomycin, epirubicin, and cisplatin for patients with locally advanced, metastatic, or recurrent undifferentiated carcinoma of the nasopharyngeal type," *Cancer*, vol. 86, no. 7, pp. 1101–1108, 1999.

[15] H. Izumi, C. Takahashi, J. Oh, and M. Noda, "Tissue factor pathway inhibitor-2 suppresses the production of active matrix metalloproteinase-2 and is down-regulated in cells harboring activated ras oncogenes," *FEBS Letters*, vol. 481, no. 1, pp. 31–36, 2000.

[16] W. R. L. Tao and Y. LIU, "Expression of Matrix Metalloproteinase-1(MMP-1) and Tissue Factor Pathway Inhibitor-2(TFPI-2) in Nasopharyngeal Carcinoma and Its significance," *Journalof-Nanchang University (Mecical Science)*, vol. 52, no. 7, p. 6, 2012.

[17] M. Xie, S. Chen, X. Xu, Z. Li, H. Shen, and J. Xu, "Preparation of two kinds of superparamagnetic carriers-supported cisplatinum complexes and the comparison of their characteristics," *Chinese Science Bulletin*, vol. 51, no. 2, pp. 151–157, 2006.

[18] H. Peng, L. Chen, J. Zhang et al., "Induction chemotherapy improved long-term outcomes of patients with locoregionally advanced nasopharyngeal carcinoma: A propensity matched analysis of 5-year survival outcomes in the era of intensity-modulated radiotherapy," *Journal of Cancer*, vol. 8, no. 3, pp. 371–377, 2017.

[19] P. S. Chen, J. L. Su, S. T. Cha et al., "promotes tumor progression by targeting the let-7 microRNA in mice and humans," *miR-107 promotes tumor progression by targeting the let-7 microRNA in mice and humans*, vol. 127, no. 3, pp. 1116-1116, 2017.

[20] S. J. An, Y. S. Huang, Z. H. Chen et al., "Lower Ras expression as an independent predictor of patient outcomes in lung cancer treated with bevacizumab plus chemotherapy," *Cancer Gene Therapy*, vol. 21, no. 3, pp. 110–114, 2014.

[21] N. Senzer, J. Nemunaitis, D. Nemunaitis et al., "Phase i study of a systemically delivered p53 nanoparticle in advanced solid tumors," *Molecular Therapy*, vol. 21, no. 5, pp. 1096–1103, 2013.

[22] T. Liu, W. Xue, B. Ke, M.-Q. Xie, and D. Ma, "Star-shaped cyclodextrin-poly(l-lysine) derivative co-delivering docetaxel and MMP-9 siRNA plasmid in cancer therapy," *Biomaterials*, vol. 35, no. 12, pp. 3865–3872, 2014.

[23] T. Liu, X. Wu, Y. Wang et al., "Folate-targeted star-shaped cationic copolymer co-delivering docetaxel and MMP-9 siRNA for nasopharyngeal carcinoma therapy," *Oncotarget* , vol. 7, no. 27, pp. 42017–42030, 2016.

[24] S.-J. Sung, S. H. Min, K. Y. Cho et al., "Effect of polyethylene glycol on gene delivery of polyethylenimine," *Biological & Pharmaceutical Bulletin*, vol. 26, no. 4, pp. 492–500, 2003.

[25] S. Mitra, U. Gaur, P. C. Ghosh, and A. N. Maitra, "Tumour targeted delivery of encapsulated dextran-doxorubicin conjugate using chitosan nanoparticles as carrier," *Journal of Controlled Release*, vol. 74, no. 1–3, pp. 317–323, 2001.

[26] F. Kohori, M. Yokoyama, K. Sakai, and T. Okano, "Process design for efficient and controlled drug incorporation into polymeric micelle carrier systems," *Journal of Controlled Release*, vol. 78, no. 1-3, pp. 155–163, 2002.

[27] A. K. Gupta and M. Gupta, "Synthesis and surface engineering of iron oxide nanoparticles for biomedical applications," *Biomaterials*, vol. 26, no. 18, pp. 3995–4021, 2005.

[28] C. S. S. R. Kumar and F. Mohammad, "Magnetic nanomaterials for hyperthermia-based therapy and controlled drug delivery," *Advanced Drug Delivery Reviews*, vol. 63, no. 9, pp. 789–808, 2011.

[29] S. Louguet, A. C. Kumar, G. Sigaud, E. Duguet, S. Lecommandoux, and C. Schatz, "A physico-chemical investigation of poly(ethylene oxide)-block-poly(l-lysine) copolymer adsorption onto silica nanoparticles," *Journal of Colloid and Interface Science*, vol. 359, no. 2, pp. 413–422, 2011.

[30] Q. He, J. Zhang, J. Shi et al., "The effect of PEGylation of mesoporous silica nanoparticles on nonspecific binding of serum proteins and cellular responses," *Biomaterials*, vol. 31, no. 6, pp. 1085–1092, 2010.